Indian Journal of Engineering & Materials Sciences
Vol. 31, December 2024, pp. 899-908
DOI: 10.56042/ijems.v31i6.10211

Design and Development of Bot using Theo Jansen Mechanism

Nilaj Deshmukh*, Ben Johnson, Earl Fernandes, Pawan Gole, & Jamshed Khan

Department of Mechanical Engineering, Fr. C. Rodrigues Institute of Technology Vashi, Navi Mumbai 400 703, India

Received: 05 April 2024; accepted: 19 November 2024

Unlike human being's bots never get tired, they can be replaced or be swapped and can be used for multiple purposes. Legged robots can be utilized for space missions on extra-terrestrial planets and in risky places. Low power consumption and weight are further advantages of walking robots, so it is important to use the minimum number of actuators. The objective is to design and fabrication of prototype of the Theo-Jansen four leg strolling robot. The essential Theo Jansen device is a 13-bar framework that strolls when a crank is rotated. The central 'crank' link moves in circles as it is actuated by a rotary actuator. All other links and pin joints are unactuated and will move because of the motion imparted by the crank. It may be utilized as a military robot by a few modifications on it such as Guns, Radar, GPS, etc. Where military rangers cannot go, it may be utilized as a surveillance bot. Developed bot is radio frequency controlled and effectively designed for low speed and based on requirement speed can be increased by using higher speed motor.

Keywords: Legged, Prototype, Robots, Surveillance, Theo-Jansen mechanism

1 Introduction

It is documented that animals can travel over rough terrain at speeds much greater than those possible with wheeled or tracked vehicles. Even a person's being, by "getting down on all fours" if necessary, can travel or climb over terrain which is impossible for a wheeled or self-propelled vehicle. It is therefore of considerable interest to find out what machines for land locomotion can do if they're designed to imitate nature[1]. Theo Jansen's mechanism, designed by Theo Jansen to simulate a smooth walking motion. Theo Jansen has used his mechanism in different kinds of kinetic sculptures which are known as Strandbeests[2]. There are many types of leg mechanisms such as Eight-bar leg mechanism, Strandbeests (applied Jansen linkage), Tokyo Institute of Technology walking chair, Ghassaei Linkage Tchebyshevs plant grade machine. But out of them, Klann mechanism and Jansen mechanism are most popular and are considered best in design[2].Theo Jansen Mechanism Model is a mechanism that can be actuated with only one motor, where input torque is driven to driving link. And, the driving link is constrained on origin of the Descartes coordinates[1].

There were lot of drawbacks of Klann mechanism, the drawbacks being jerky motion and difficulty in the turning of the vehicle. The next step to be taken was to find a better mechanism which had a smooth walking pattern on any given terrain and could easily function as per requirements. The most flexible mechanism better than Klann mechanism was Theo-Jansen mechanism[3]. When two Jansen linkages are connected to each other by a rotating horizontal shaft, both the legs help the machine to move forward or backward depending on the clockwise or anticlockwise rotation of the shaft[4].

Interestingly, the relationship of the hind limb with the fore limb is antiphase, thus helping them to move forward cooperatively. The parallel link in the Jansen linkage helps the linkage to attain the required step height by folding during the cycle angling of the leg. The Jansen linkage is a closed chain linkage. Though this would handicap the machine to some degree but it significantly reduces the number of actuators and is suitable enough for multiple applications[4].

A detailed study of this robot has been done by Patnaik[3]. This study explored and analysed the Jansen linkage as a permanent replacement for the wheels of load carrying tippers and trucks used in mining. The main aim of his research was to remove the problems associated with the smooth movement of vehicles at mining sites, which is commonly dealt with by making roads separately for it, a time consuming and costly process. Other applications include Crab-type Robot, Amphibian-legged robot, Sports ground/pitch-marking robot, Robot for stage performance, Pitch-Marking Robot, Pitch-Marking Robot, Mei-Mei robot, Stair-climbing robot, Strand beests and Lion-type robot[4-9].

*Corresponding author (E-mail: nilaj.deshmukh@fcrit.ac.in)

This paper describes a new economical solution of robot control systems. The presented robot control system can be used for different sophisticated robotic applications. The system uses a bot which is capable of walking towards the object according to the user remote control. This paper discussed the design and fabrication of a Mechanical walker robot using the wireless remote. As it is a wireless Robot it can be easily mobilized and can be controlled. In this prototype a micro controller was used, which was programmed to control the input and output modules interfaced to it. The controller makes use of a remote, which is used to control the robot. The prototype consists of micro controller-based motherboard which is present with the Robot itself. It is interfaced with some DC motors for moving the robot, and a RF module for receiving the instructions from the remote. Also the analysis study was done to understand the variation acceleration and stress analysis on the leg and flat bed of the bot was carried out in order to understand the durability of the Bot.

2 Materials and Methods

Walking machines possess several advantages over wheeled machines in areas of variable terrain. Consider a wheel moving a constant velocity V; every point on its perimeter is moving at a constant velocity V tangent to the curve of the wheel as shown in Fig. 1.

A comparable walking mechanism would be one which moves at a constant velocity V, and where the "foot" of the walker traces out a similar circular path with a constant velocity V at all points on the path (also shown in Fig. 1). The most obvious advantage of the foot over the wheel is that the foot may step over inconsistencies in the terrain. Local maxima and minima may be completely avoided by simply stepping over them. This results in less loss of energy during locomotion and allows the vehicle to maintain a constant velocity and height over variable terrain.

The dotted lines indicate the perimeter of the wheel or the path of the foot. The arrows indicate the direction of movement. The foot may step over the obstacle completely, while the wheel must move over the obstacle. Now consider a case where the comparable foot and wheeled systems approach an obstacle that cannot be avoided, as shown in Fig. 2.

When the edge of the wheel makes contact with the higher ground, it forces the velocity of the vehicle to immediately slow. This edge has a total velocity V, but only a fraction of that velocity is in the x direction, so the vehicle quickly slows from V to Vx2. The foot encounters a similar change in velocity, but it has the advantage of being able to slide along the ground. Although this scenario is not ideal, dragging the front foot across the raised terrain reduces change of velocity in the x direction. Both

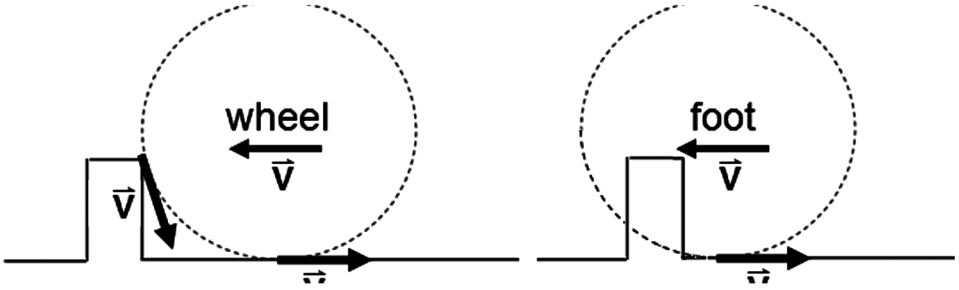

Fig. 1 — Comparison of wheel and foot response to a local maximum in the terrain[5].

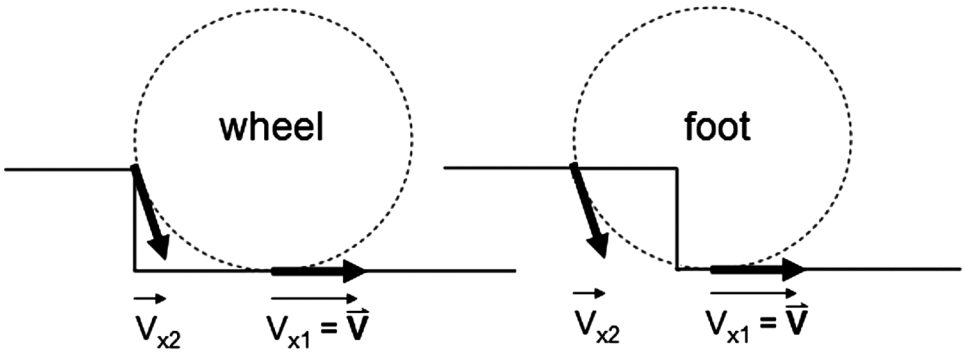

Fig. 2 — Comparison of a wheel and a foot (moving in a wheel-like path)[5].

models must still overcome the potential energy barrier posed by the increased height of the terrain.

A comparison of a wheel and a foot (moving in a wheel-like path) approaching an inconsistency in the terrain. The x component of the velocity of the edge of the wheel and the foot's path are indicated. Furthermore, the wheel causes a great deal of environmental harm. Its inability to avoid obstacles means that it erodes more terrain than a foot when moving comparable 3 vehicles. Additionally, wheeled vehicles work best on terrain with no inconsistencies; this has led to paving of many permanent roadways, another form of environmental degradation. The benefits of walking over rolling on rough terrain are summed up in the following: Higher energy efficiency, better fuel economy, Increased speed, Greater mobility, Improved isolation from terrain inconsistencies, less environmental damage (both from paving and erosion).

2.1 Design

Several structural design considerations should be taken into account for economical and efficient manufacturing. Many of these apply to other joining methods, and all apply to both subassemblies and the complete structure. The device should be suitable for local manufacturing capabilities. The attachment should employ low-cost materials and manufacturing methods. It should be accessible and affordable by low-income groups, and should fulfil their basic need for mechanical power. It should be simple to manufacture, operate, maintain and repair. It should be as multi-purpose as possible. Standard steel pieces such as steel plates, iron rods, angle iron, and flat stock that are locally available should be used. Excessive weight should be avoided, as durability is a prime consideration. Major aspects during design consideration also include Strength, Rigidity, Reliability, Safety, Cost, Weight, Ergonomics, Aesthetics, Manufacturing considerations, Assembly considerations, Conformance to standards, Friction and wear, Life, Vibrations, Thermal considerations, Lubrication, Maintenance, Flexibility, Size and shape, Corrosion, Noise and Environmental considerations. In order to design our bot we took into account that our robot design should be aesthetics, Hence the aesthetic considerations were, Form(shape), Symmetry and shape, Colour, Continuity, Variety, Proportion, Noise, Contrast and purpose, Style, Material and surface finish, Tolerance etc.

2.1.1 3D model

After carefully examination of the research papers, the dimensions were finalised. Keeping all the design considerations in mind the accurate lengths of the links were given. The length of the links is in terms of the aspect ratios respective of its crank mechanisms[6].

Figure 3 is the dimensions of the links and various parts of our 3D model made on the drawing sheet of the Solid works software. It has the detailed dimensional information about the legs and gear pitch etc.

Figure 4 is the 3D model developed on solid works. After completion of the Dimensional aspects the Aesthetic considerations were kept in mind and the 3D model was developed. Figures 5, 6 & 7 are the different set of views of the same 3D model. All those figures give us the accurate positioning of the different components in the bot. The information Regarding the placing of the leg, gears and flat-bed plate is properly visible in the figures. As you can see in the above-mentioned figures, we have provided a flat-bed to attach any surveillance tool (e.g.-Camera).

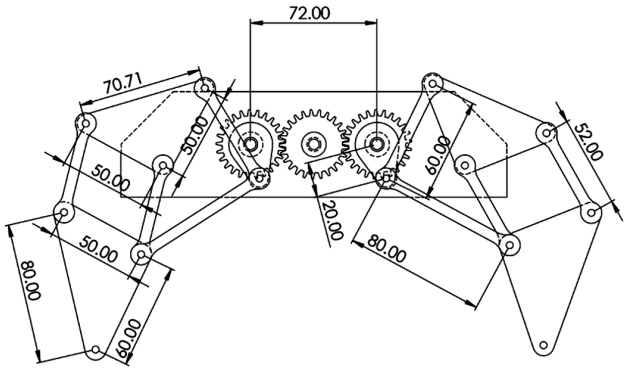

Fig. 3 — Dimensions of the various parts of the 3D model.

Fig. 4 — 3D View of 3D model made on solidworks software.

As you can see in the figures there are 4 pairs of legs for locomotion.

2.1.2 Development of remote control

Transmitter Circuit - In Fig. 8 the HT12E encoder IC VSS pin is connected to the power supply Ground (-) and the VDD is connected to the power supply VCC (+). IC A0 – A7 pins (pin 1 – 8) are connected to the Ground(-) to set the address at 0b00000000. The Switch 1 (S1), Switch 2 (S2), Switch 3 (S3), and Switch 4 (S4) are respectively connected to the AD11 (13), AD10 (12), AD9 (11), and AD8 (10). The 1M ohm resistor is connected between the pin 15 and 16, which provides the external resistance for the operation of the internal oscillator of the HT12E IC. The RF Transmitter module GND pin is connected to the power supply Ground (-) and the VCC is connected to the power supply VCC (+). The Data pin is connected to the DOUT (pin 17) of the IC[7].

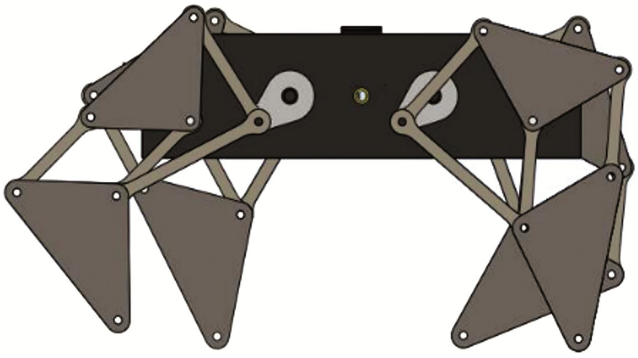

Fig. 5 — Side view of 3D model.

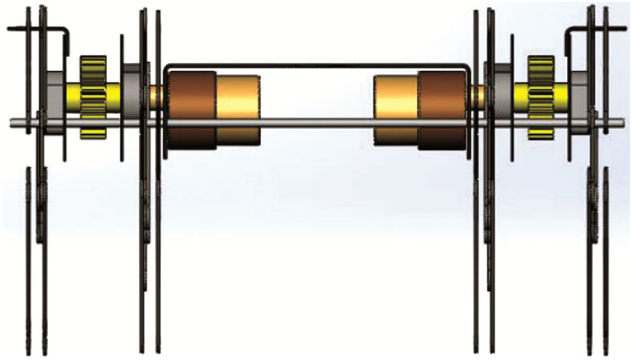

Fig. 6 — Front view of 3D model.

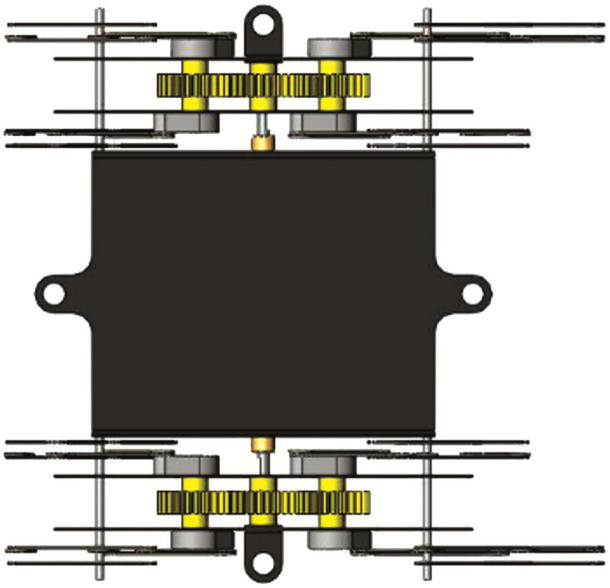

Fig. 7 — Top view of 3d model.

Receiver Circuit - In Fig. 9 the HT12D decoder IC VSS pin is connected to the power supply Ground (-)

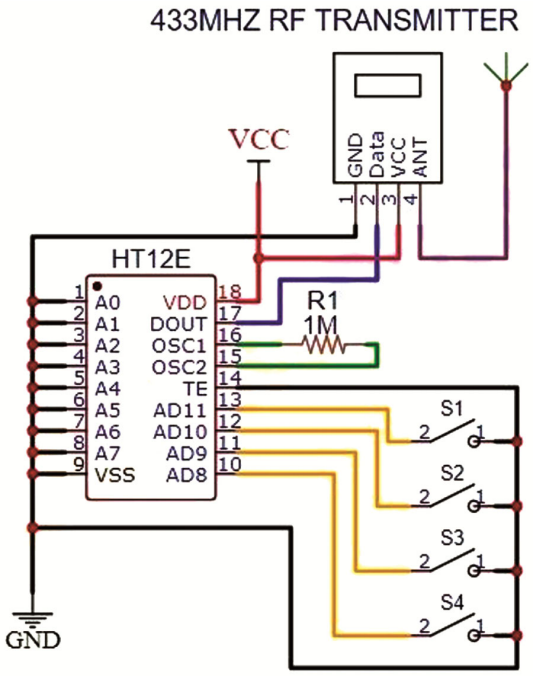

Fig. 8 — 433 MHz RF transmitter circuit diagram[7].

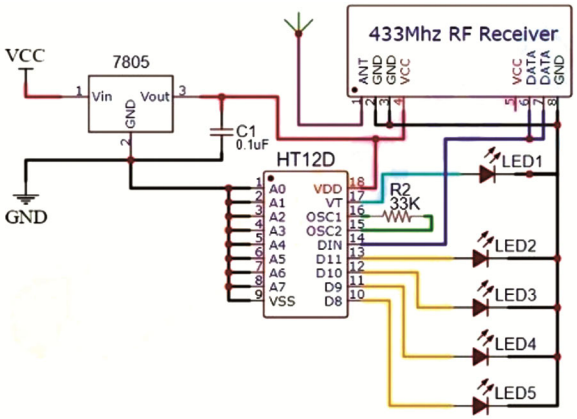

Fig. 9 — 433 MHz RF receiver circuit diagram[7].

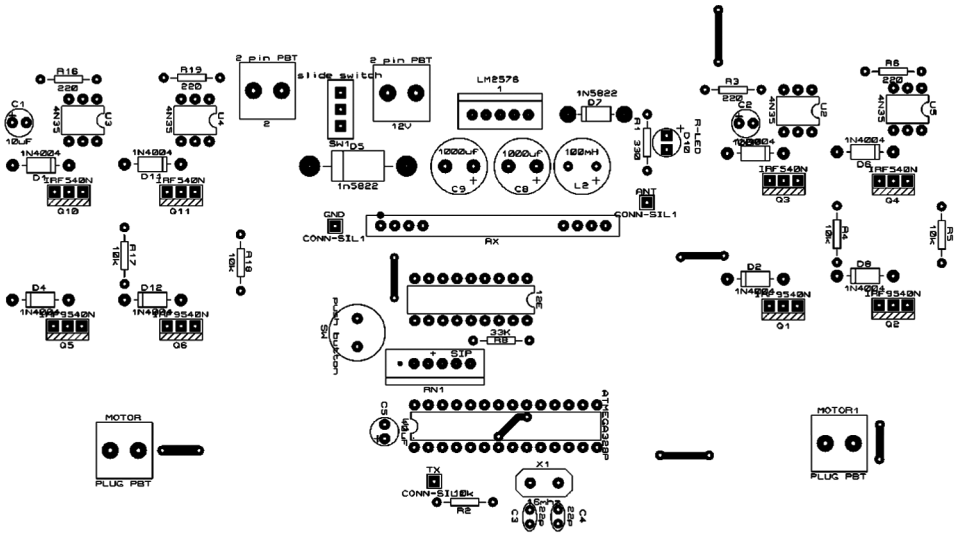

Fig. 10 — PCB layout of receiver module.

and the VDD is connected to the power supply Vout (+) of the 7805 5v voltage regulator. IC A0 – A7 pins (pin 1 – 8) are connected to the Ground(-) to set the address at 0b00000000. The LED2, LED3, LED4, and LED5 are respectively connected to the D11 (13), D10 (12), AD9 (11), and D8 (10). The 33K ohm resistor is connected between pin 15 and 16, which provides the external resistance for the operation of the internal oscillator of the HT12D IC. The RF Receiver module GND pins are connected to the power supply Ground (-) and the VCC is connected to the power supply VCC (+). The Data pin is connected to the DIN (pin 14) of the IC[7].

Working of RF Transmitter and Receiver Circuits - In Fig. 8 and 9 the HT12E encoder IC's 4 data pins are connected to the 4 push buttons. The push buttons provide 4-bit data to the HT12E encoder IC. Then the IC converts these 4-bit data into serial data and this serial data will be available at the DOUT pin (pin17) of the IC. This output serial data is given to the RF Transmitter module. Then the RF transmitter module transmits this serial data using radio signals. At the receiver side, the RF receiver module receives this serial data coming from the transmitter. Then this serial data is given to the DIN pin (14) of the HT12D Decoder IC. Now the decoder IC will convert the received serial data into 4 bit parallel data. The 4 data pins of the decoder IC are connected to 4 LEDs, which is control according to the transmitted data from the transmitter. When connected with Power supply to both circuits and we should notice that all LEDs will start glowing. Because the push-button pins (IC pin D8-D11) are pulled up internally by the Encoder IC. If we will press one push-button the data

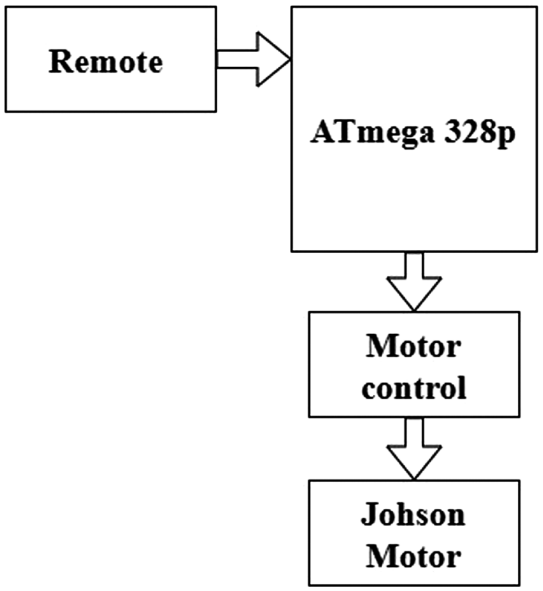

Fig. 11 — Flow chart of process.

pin is connected to the ground in the transmitter circuit, then the respective LED will be turned off in the receiver circuit. For example, if we will press Switch 1 (S1) which connected to the AD11 (pin13) of the Encoder IC, then the LED 2 will turn off which is connected to the D11 (pin13) of the Decoder IC[7].

In Fig. 10 and Fig. 11 the circuit uses standard power supply comprising of a step-down transformer from 230Vto 12V and 4 diodes forming a bridge rectifier that delivers pulsating dc which is then filtered by an electrolytic capacitor of about 470µF to 1000µF. The filtered dc being unregulated, IC LM7805 is used to get 5V DC constant at its pin no 3 irrespective of input DC varying from 7V to 15V. The

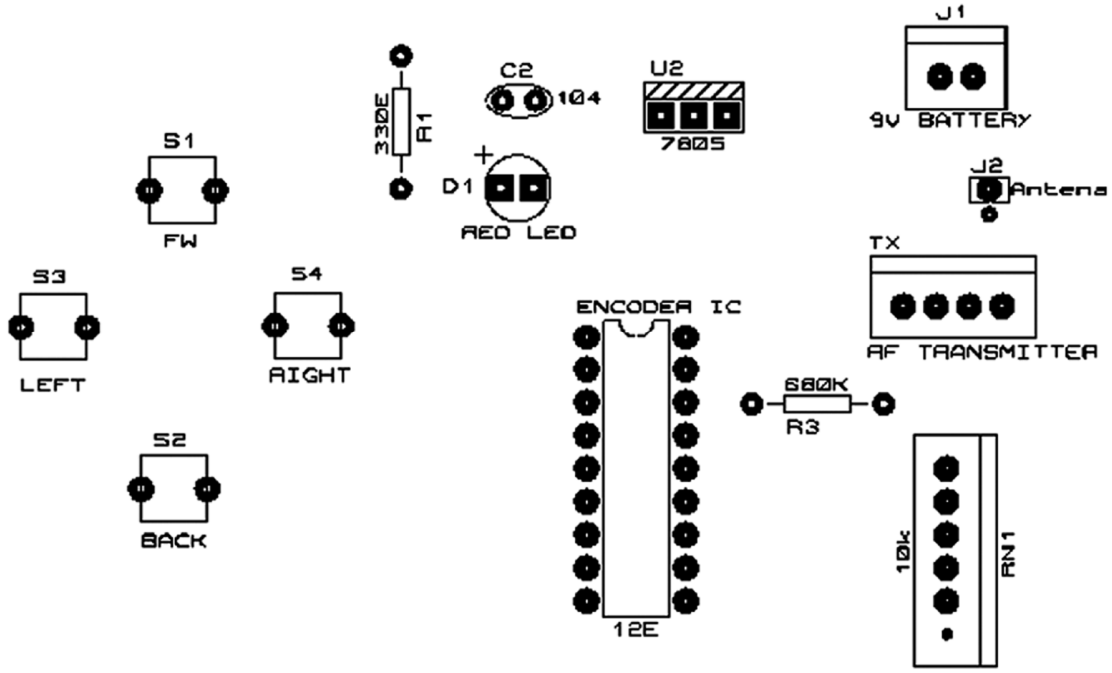

Fig. 12 — PCB layout of remote control.

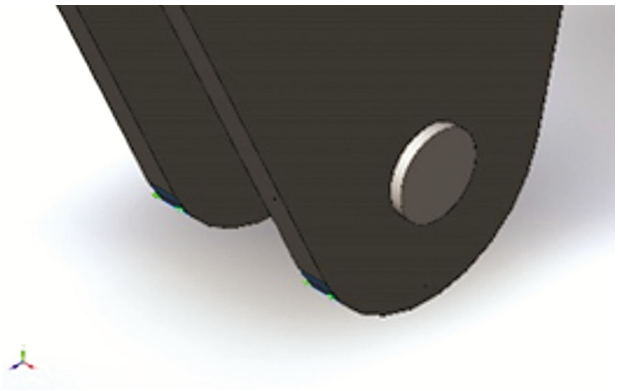

Fig. 13 — Bottom of leg (contact point of the bot with the ground).

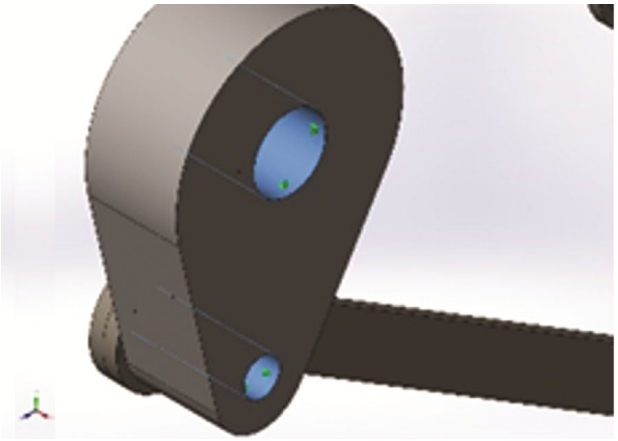

Fig. 14 — Fixed hinge.

input dc shall be varying in the event of input ac at 230volts section varies from 160V to 270V in the ratio of the transformer primary voltage V1 to secondary voltage V2 governed by the formula V1/V2=N1/N2. As N1/N2 i.e. no. of turns in the primary to the no. of turns in the secondary remains unchanged V2 is directly proportional to V1. Thus, if the transformer delivers 12V at 220V input it will give 8.72V at 160V.Similarly at 270V it will give 14. 72V.Thus the dc voltage at the input of the regulator changes from about 8V to 15V because of A.C voltage variation from 160V to 270V the regulator output will remain constant at 5V.

The regulated 5V DC is further filtered by a small electrolytic capacitor of 10μF for any noise so generated by the circuit. One LED is connected of this 5V point in series with a current limiting resistor of 330Ω to the ground i.e., negative voltage to indicate 5V power supply availability. The unregulated 12V point is used for other applications as and when required.

Based on Fig. 10 and Fig. 12 the different components of the Receiver Module and the remote control are shown. Based on these PCB layouts the fabrication was carried out.

3 Results and Discussion

3.1 Analysis of leg

Figures 13, 14, 15 & 16 are the different types of static stress, strain, displacement etc. analysis carried

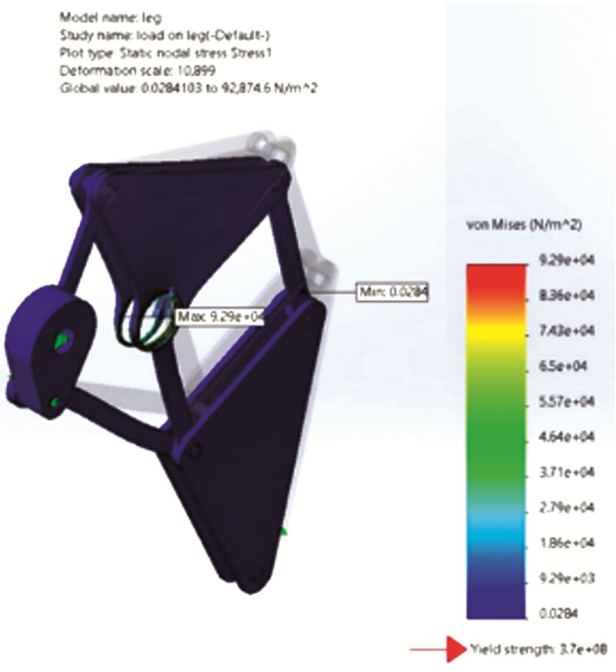

Fig. 15 — Stress analysis on leg.

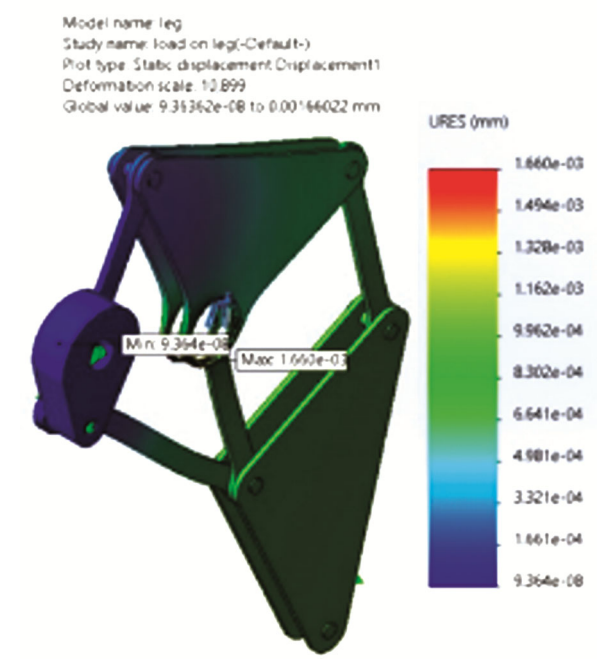

Fig. 16 — Static displacement of leg.

out on the leg of the robot using Solid Works software. Fig. 13 and Fig. 14 represents the magnitude of reactive forces on the fixed support of the leg. The magnitude of Initial loading conditions for analysis was taken as 1 Kg i.e. 9.81 N.

(a) According to Fig. 13, Forces of Reaction on the bottom of the Leg are,

$R_x = 2.78287 \times 10^{-6}$ N ... (1)

$R_y = 1.15717 \times 10^{-9}$ N ... (2)

$R_z = -1.18749 \times 10^{-8}$ N ... (3)

$\therefore$ Resultant, $R = 2.78289 \times 10^{-6}$ ... (4)

(b) According to Fig. 14, Forces of Reaction on the Fixed Hinge are,

$R_x = -2.77829 \times 10^{-6}$ N ... (5)

$R_y = -5.67798 \times 10^{-9}$ N ... (6)

$R_z = 2.46373 \times 10^{-8}$ N ... (7)

$\therefore$ Resultant, $R = 2.7784 \times 10^{-6}$ ... (8)

(c) The Stress analysis was carried on the leg-

According to Fig. 15, we can see the different sections of the leg under stress conditions. The parts of the leg with more stress concentration can be shown using von misses stress plot. Hence the section with the Maximum concentration of stress and the section with the minimum concentration of stress are shown the Fig. 15.

$\therefore$ Max = 9.29×10^4 N/m^2 ... (9)

$\therefore$ Min = 0.0284 N/m^2 ... (10)

(d) The Strain analysis was carried on the leg-

The parts of the leg with more Strain concentration can be shown using equivalent strain plot (ESTRN). Hence the section with the Maximum concentration of strain and the section with the minimum concentration of strain .

$\therefore$ Max = 3.284×10^4 N/m^2 ... (11)

$\therefore$ Min = 2.421×10^{-1} N/m^2 ... (12)

(e) The Displacement analysis was carried on the leg-

According to Fig. 16 we can see the Resultant Displacement of the leg. The parts of the leg with more resultant displacement can be shown using the URES plot. Hence the section with the Maximum Displacement and the section with the minimum Displacement are shown the Fig. 19.

$\therefore$ Max = 1.660×10^{-3} N/m^2 ... (13)

$\therefore$ Min = 9.364×10^{-3} N/m^2 ... (14)

3.2 Analysis of plate

Figures 17 & 18 are the different types of static stress, strain, displacement etc. analysis carried out on the flat bed plate of the robot using Solid Works software.

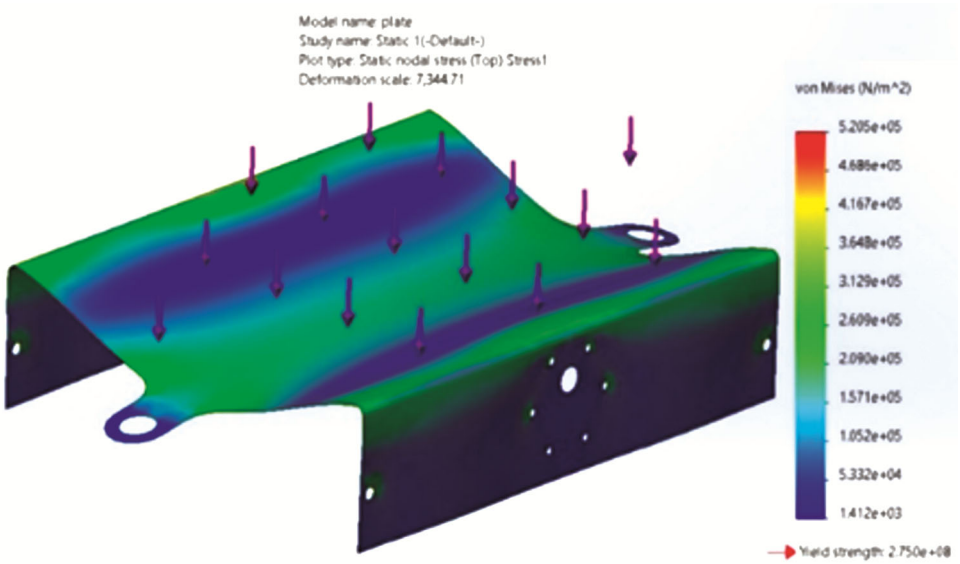

Fig. 17 — Stress analysis on plate.

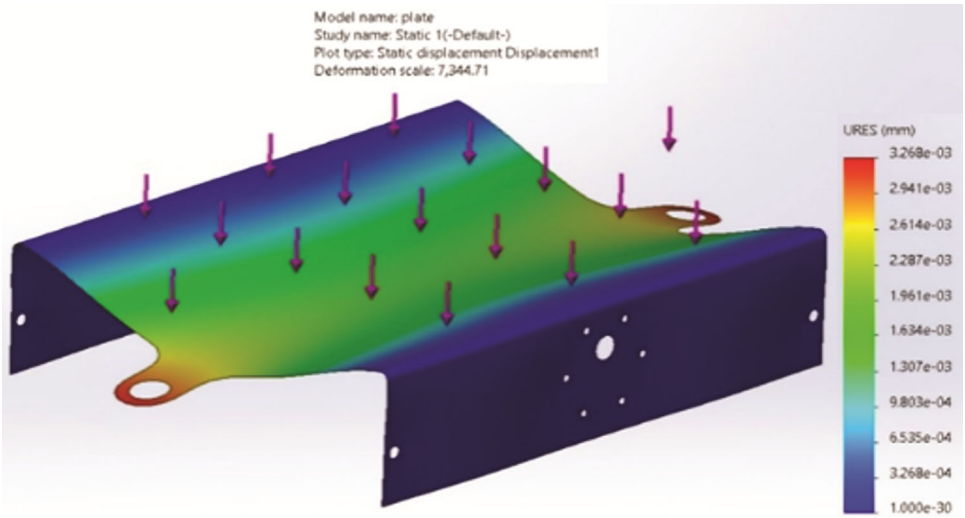

Fig. 18 — Displacement analysis on plate.

(a) The Stress analysis was carried on the flat bed plate-

According to Fig. 17 we can see the different sections of the plate under stress conditions. The parts of the plate with more stress concentration can be shown using von misses stress plot. Hence under uniformly distributed load conditions the deformation of the plate was observed.

(b) The Strain analysis was carried on the flat bed plate-

The parts of the plate with more strain concentration can be shown using strain plot (ESTRN). Hence under uniformly distributed load conditions the deformation of the plate was observed.

(c) The Displacement analysis was carried on the leg-

According to Fig. 19 we can see the Resultant Displacement of the flat bed plate . The parts of the plate with more resultant displacement can be shown using the URES plot. Hence the section with the Maximum Displacement and the section with the minimum Displacement are shown the Fig. 18. Hence under uniformly distributed load conditions the deformation of the plate was observed.

3.3 Fabricated protoype

This section represents the images of the developed prototype. As seen from the images the fabrication was completed.

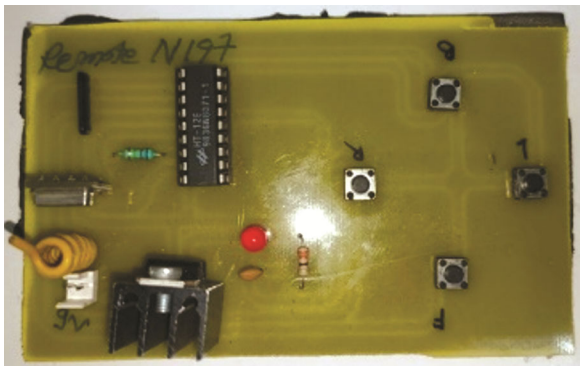

Fig. 19 — Remote control unit.

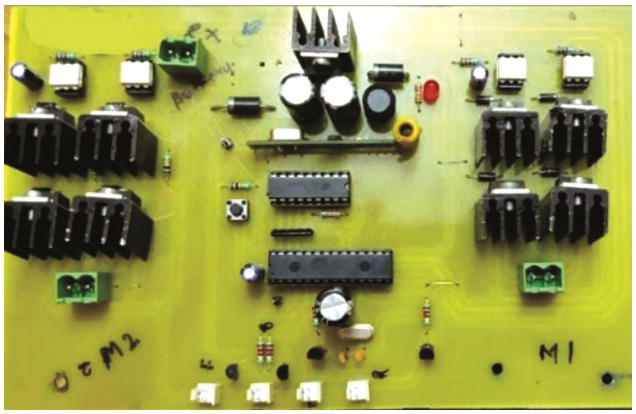

Fig. 20 — Receiver module.

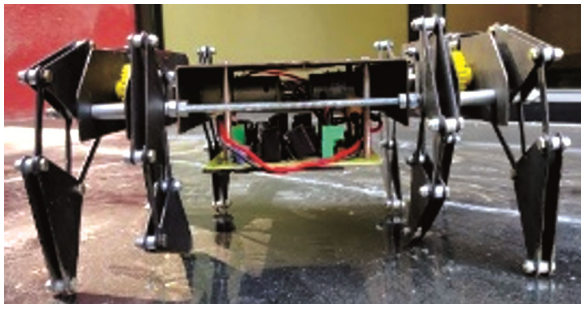

Fig. 21 — Front view of developed prototype.

Based on Fig. 12 PCB layout, the fabrication of the remote control unit was done. Fig. 19 is the fabricated remote control unit. The denotations above the buttons are to denote the movement functions of the buttons i.e. F- Front, L- Left, R- Right and B- Back. The fabrication was done using PCB machine. Similarly, based on Fig. 10 PCB layout, the fabrication of the Receiver module was done. Fig. 20 is the Fabricated receiver module.

Figures 21, 22 & 23 are the different set of views of fabricated Bot. The proper placing of the different components of the bot is clearly visible in the figures. The Receiver module is mounted on the below the flat

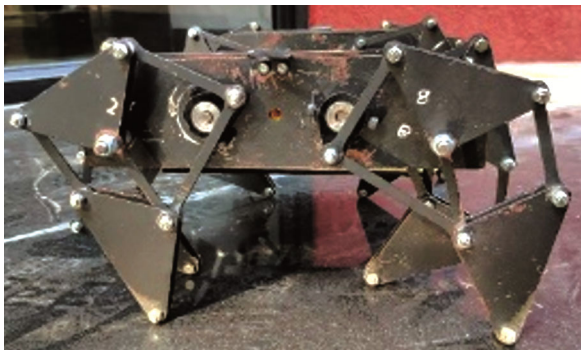

Fig. 22 — Side view of developed prototype.

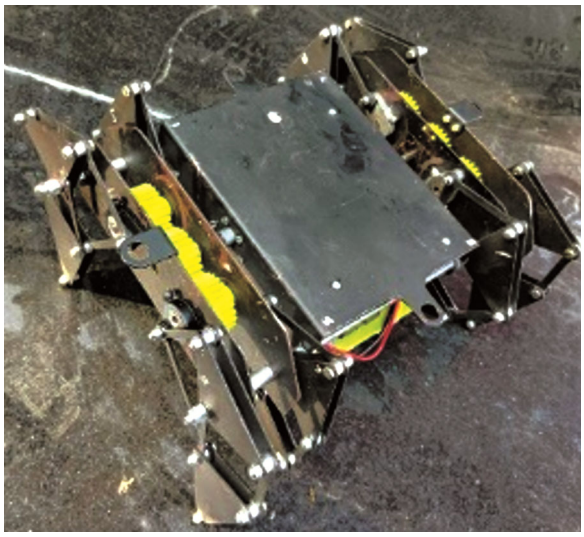

Fig. 23 — Isometric view of developed prototype.

bed plate. The metal(steel) parts of the bot were cut using laser cutting machine. The dimensions are according to the drawing sheet that was developed by us shown in Fig. 3. After keeping all design consideration and aesthetic considerations in mind, the bot was assembled and the Fabrication was completed.

4 Conclusion

This investigation showed that different elliptic circles for strolling, climbing, venturing in a place and moving back by utilizing the cyclic movement of the linkage centre. This paper is to contemplate about the Theo-Jansen 8-leg robot. This bot was able to carry about 1kg of load while demonstration process. Camera mounting or other type of load can be accommodated on the top bed of the bot as the bot consist of holes for screws or bolt, hence load is safe from toppling down. As the work of this project of was carried out, there were different types of challenges while assembling of the gears for the crank mechanism. The fixing of the gears was the most

difficult part faced while assembly of the bot. After Overcoming all those difficulties the assembly was completed. Also, the loci of the leg bottom was not as large as expected. These loci can be enlarged by using links which are larger in length. The speed of this bot is not fast but by using high speed motors and other electronic component it can be increased. Therefore, on the basis of all the previous research paper and overcoming different types of problems the 3D modelling and fabrication of this robot was completed.

References

1 PundeY, DhandeY, Chopde A & Bagade S, *Int J Eng Res Technol*, 9 (09) (2020) 42.

2 Teli1S, Agarwal R, Bagul D, Badawane P & Bandre R, *Int Res J Eng Technol*, 6 (03) (2019).

3 Patnaik S, *IOSR J Eng*, 05 (2015), 43.

4 Sengupta S & Bhatia P, *Int J Adv Res Innov*, 5 (3) (2017) 354.

5 Selvi Ö, Ceccarelli M & Yavuz S, *Adv Mech Mach Sci*, 73(2019).

6 Rao D V, Naidu A L & Kona S, *Int J Eng Trends Technol*, 47, (8), (2017)468–473.

7 Watanabe T & Iizuka K, *Int J Mech Eng Robot Res*, 9 (7) (2020) 979.

8 Widhiada W, Nindhia T, Widiyarta L & Budiarsa I, *Int J Mech Eng Robotics Res*, 9(10), (2020), 1447.

9 Özgün S &Yavuz S, *International Workshop on Computational Kinematics,* (2017).